PNAS
www.pnas.org

Supplementary Information for

A model metabolic strategy for heterotrophic bacteria in the cold ocean based on Colwellia psychrerythraea 34H

Jeffrey J. Czajka[1], Mary H. Abernathy[1], Veronica T. Benites[3,4], Edward E.K. Baidoo[3,4], Jody W. Deming[2†] and Yinjie J. Tang[1†]

[†]Corresponding authors:

Jody Deming (Phone: 206-543-0845; Email: jdeming@uw.edu)

Yinjie Tang (Phone: 314-935-3441; Email: yinjie.tang@wustl.edu)

This PDF file includes:

Metabolite abbreviations
Method details
Figs. S1 to S7
Table S1

Other supplementary materials for this manuscript include the following:

Datasets S1 and S2

www.pnas.org/cgi/doi/10.1073/pnas.1807804115

Abbreviations for metabolites

3PG(or G3P), 3-phosphoglycerate
6PG(or PG6), 6-phosphogluconate
AceCoA, acetyl-CoA
AKG, α-ketoglutarate
CIT, citrate
DHAP, Dihydroxyacetone phosphate
E4P, erythrose 4-phosphate
F6P, fructose 6-phosphate
FBP, Fructose 1,6-bisphophate
FUM, fumarate
G6P, glucose 6-phosphate
GAP, glyceraldehyde 3-phosphate
GLX, glyoxylate
ICT, isocitrate
MAL, malate
OAA, oxaloacetate
PEP, phosphoenolpyruvate
PYR, pyruvate
R5P, ribose 5-phosphate
Ru5P, ribulose-5-phosphate
S7P, sedoheptulose-7-phosphate
SUC, succinate
SucCoA, succinyl-CoA
X5P, xylulose-5-phosphate

Method Details

LC-MS analysis. Metabolite dynamic labeling samples were run on two instruments to verify at the Joint Bioenergy Institute (JBEI) and the Donald Danforth Plant Center. Metabolites were extracted in 6:4 MeOH:chloroform at –4°C, with samples shaken at 300 rpm and vortexed every hour for four hours. After addition of 0.5 mL of ddH2O, the samples were centrifuged. The upper aqueous phase was extracted twice and centrifuged for 90 minutes in 3KDa filters at 0°C. Samples were then frozen, lyophilized, and reconstituted. LC-MS sample runs, analysis, and data extraction were performed at the Joint Bioenergy Institute (JBEI) and the Donald Danforth Plant Center. JBEI samples were reconstituted in 100 µL of 60% acetonitrile, 15% methanol and 25% ddH2O and

were run according to the previously published protocol (1) with these differences: the mobile phase was changed to 20 mM ammonium carbonate (Sigma-Aldrich, St. Louis, MO, USA) in water (solvent A) and 20 mM ammonium carbonate in 70% acetonitrile and 30% water (solvent B); the column compartment was set to 40°C; and the liquid chromatography gradient was linearly decreased from 100% B to 70% B in 9 minutes, decreased from 70% B to 60% B in 2.8 minutes, increased from 60% B to 100% B in 0.2 minutes, and held at 100% B for a further 10 minutes. The total LC run time was 22 minutes. A flow rate of 0.2 mL minute–1 was used throughout. Samples run at the Donald Danforth Plant Center were reconstituted in 100 µL of ddH2O, and run as according to the previously published protocol (2).

Thermodynamic calculations. The ionic strength of the ASW medium was calculated from equation 1:

$$I = \frac{1}{2} \sum_{i=1}^{n} C_i * Z_i^2 \qquad \textbf{(1)}$$

where I is the ionic strength in (M), C_i is the concentration of the dissociated species, and Z_i is the charge of the dissociated species. The change in Gibb's free energy formula (equation 2) was used to estimate the change of free energy from standard temperature to 4°C:

$$\Delta G = -R * T \ln(K_{eq}) \qquad \textbf{(2)}$$

where R is the ideal gas constant, T is the temperature, and K_{eq} is the equilibrium constant.

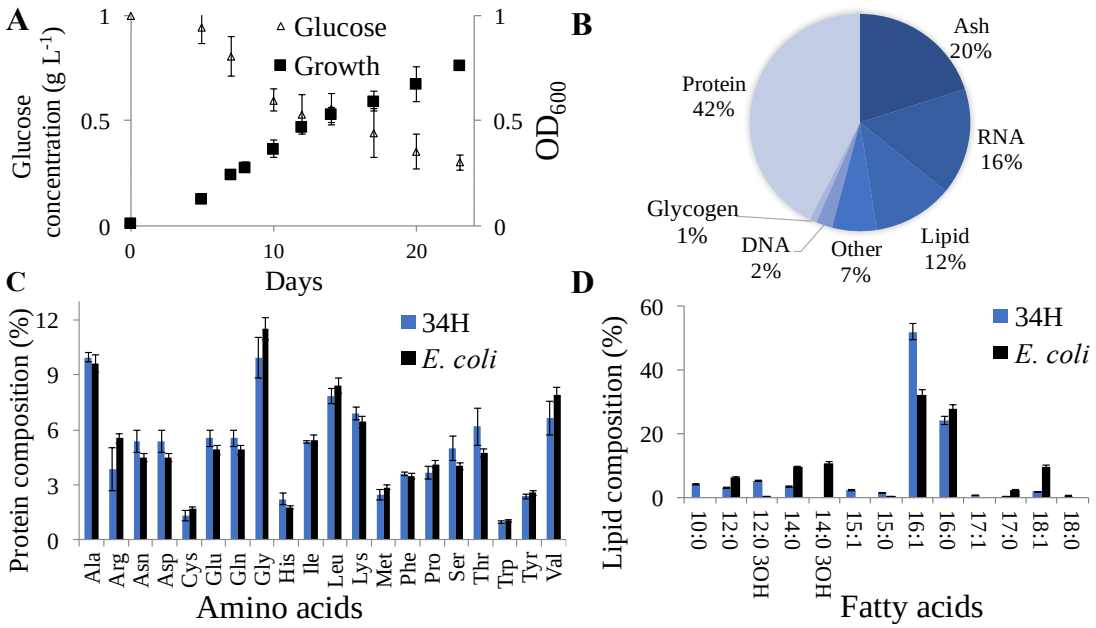

Fig. S1. Physiological characterization of 34H on glucose at 4°C to establish a basis for developing a dynamic view of its metabolism at this normal-growth temperature. (*A*) Growth rate by optical density (OD_{600}) and glucose consumption (by enzymatic assay) in defined minimal marine medium. (*B*) Biomass composition, where percentage of ash represents inorganic salts, and nucleic acid percentages were estimated from the ratio of protein to DNA/RNA in *E. coli* (3, 4). (*C*) Protein composition, with comparative amino acid percentages for *E. coli* at its normal-growth temperature of 37°C (5). (*D*) Lipid profile, similarly compared to *E. coli*. Error bars indicate standard deviation of the mean (n = 3).

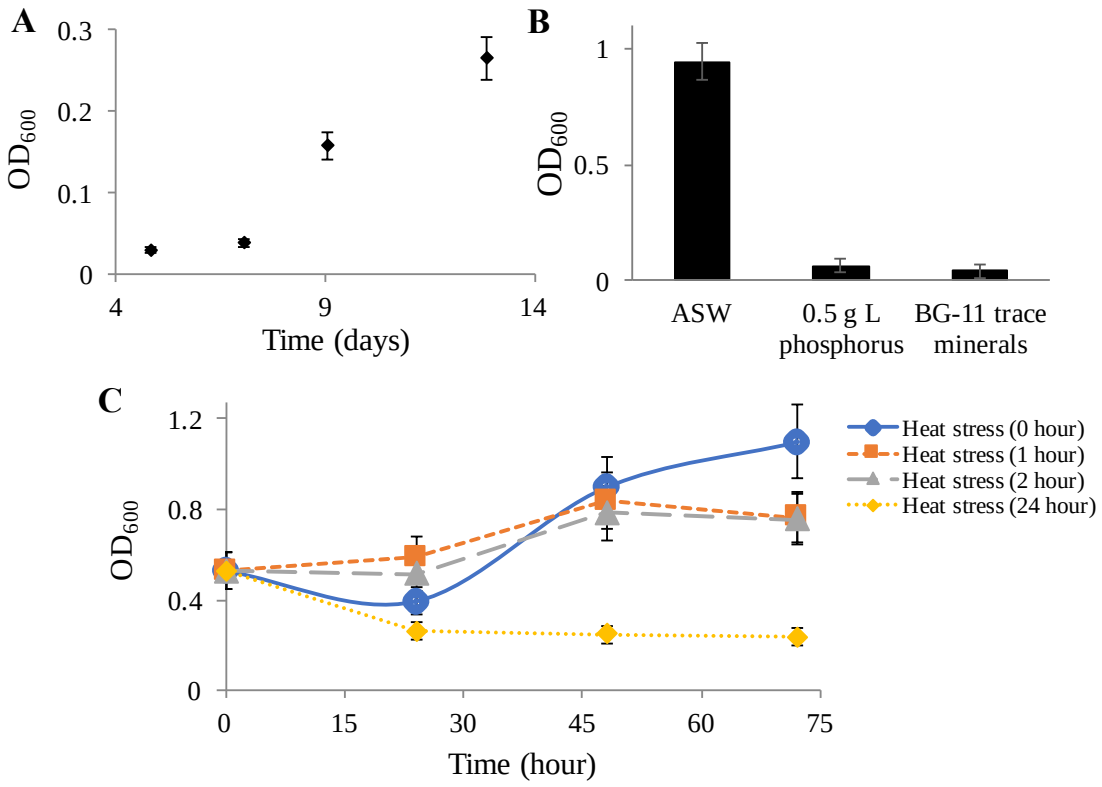

Fig. S2. Growth profiles of 34H based on optical density (OD_{600}). (*A*) Growth curve in ASW minimal media supplemented with lactate (1 g L^{-1}). (*B*) Final OD_{600} of 34H grown in ASW minimal media supplemented with glucose (1 g L^{-1}) and either additional glucose (0.5 g L^{-1}) or BG-11 trace minerals. (*C*) Growth curves in complex media at 4°C after exposing cultures to room temperature (heat stress) for 0, 1, 2 and 24 hours.

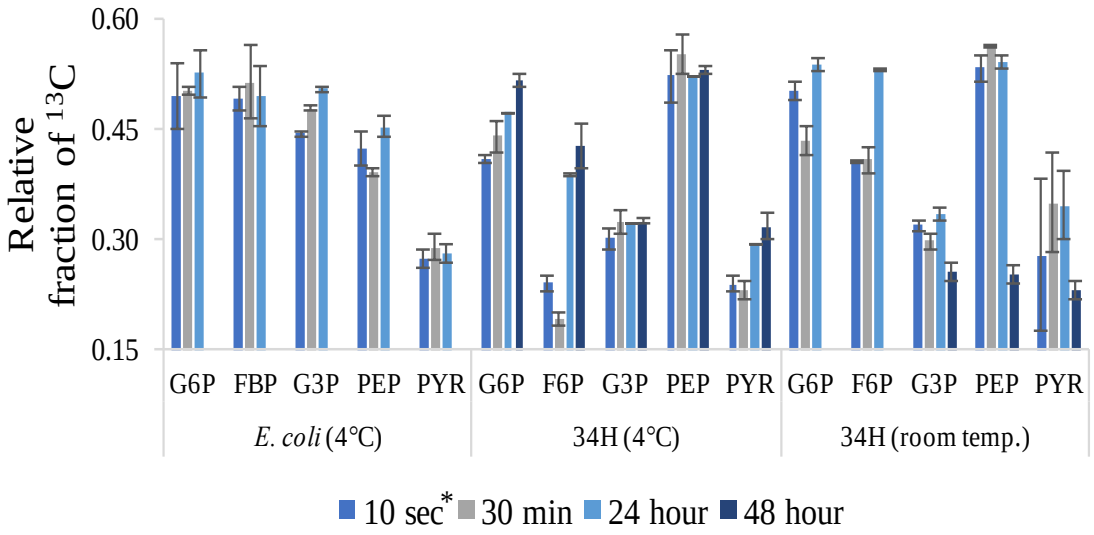

Fig. S3. Dynamic labeling experiments with *E. coli* and 34H conducted with U-^{13}C glucose at 4°C (*E. coli* and 34H) and at room temperature (34H). Comparison of metabolic labeling responses of glycolytic metabolites in cold-stressed (4°C, following acclimation at 4°C for 1 hour) *E. coli*, normal-growth 34H (4°C), and heat-stressed 34H (room temperature, following acclimation for 1 hour). *E. coli* was not sampled at 48 hours; G6P and F6P were not detected in 34H room-temperature samples at 48 hours. For 10-sec data (asterisk), cell metabolism may have been active during the 5-minute centrifugation (0°C) step. Error bars indicate standard deviation of the mean (n = 2).

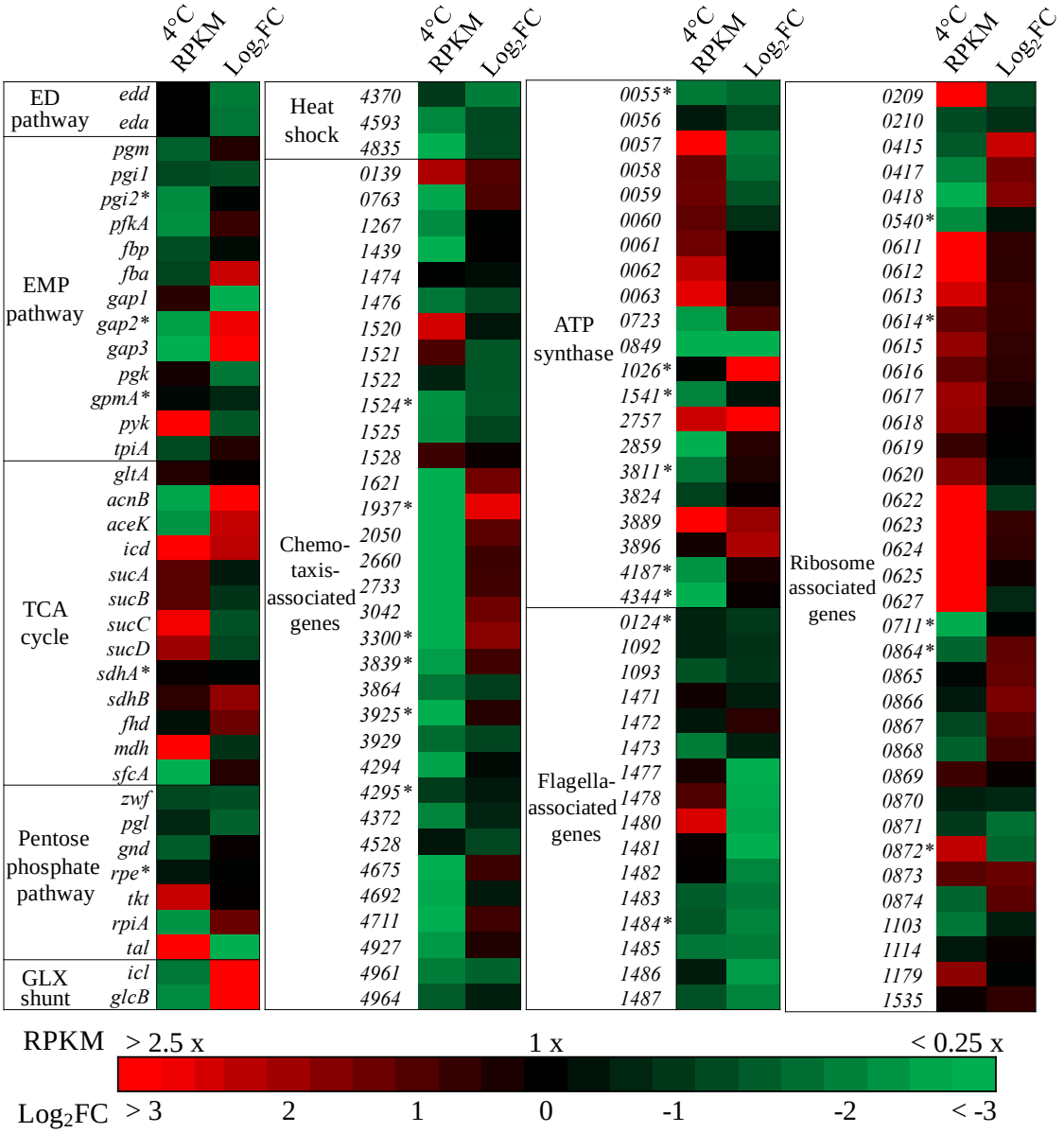

Fig. S4. Transcriptomic expression data of 34H at normal-growth conditions and differential expression data after exposure to temperature-stressed conditions as determined by RNA-Seq. Left column represents RPKM expression levels normalized to gene edd-1 (ED pathway). Right column represents Log_2(FoldChange) (Log_2FC) of differential gene expression from 4°C to 23°C. Scale for RPKM expression and Log_2FC presented on the far right. An asterisk next to gene names indicates data with Log_2FC Benjamini-Hochberg FDR adjusted p-values less than 0.05. See *SI Appendix*, Dataset S2 for full gene expression details.

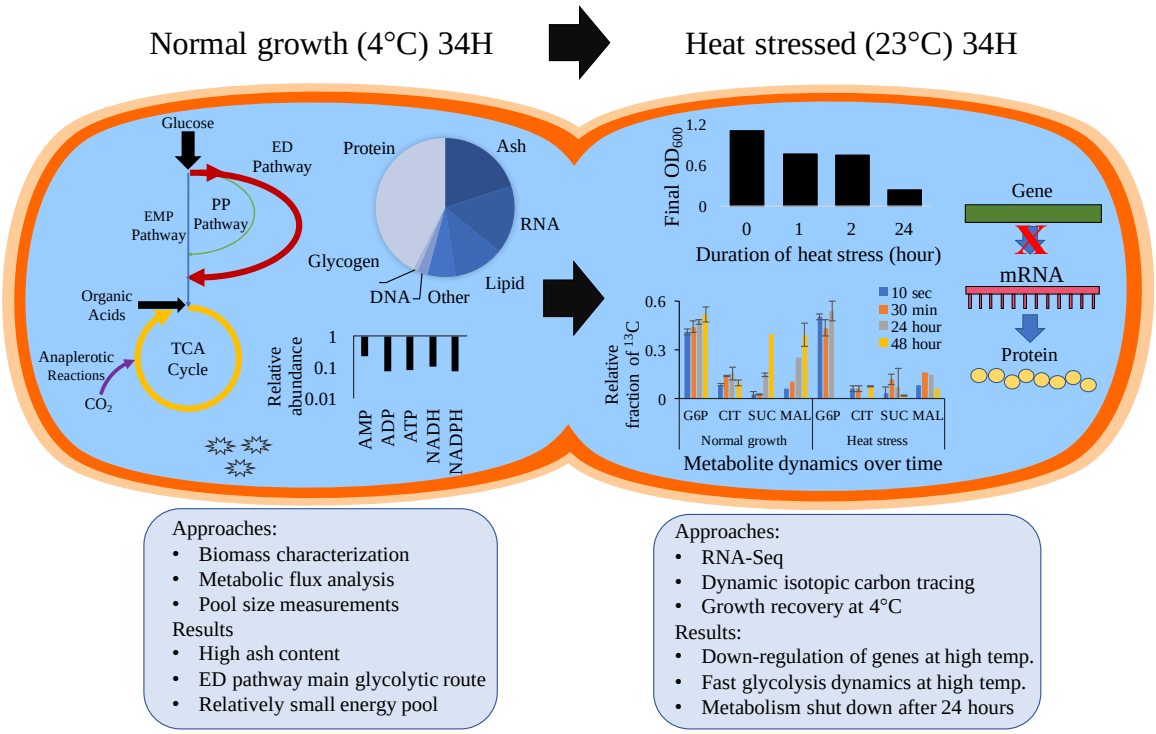

Fig. S5. Overview of experimental approaches and key findings for 34H at temperatures for both normal-growth (4°C) and heat-stress (23°C, above its maximum growth temperature). The left side shows experimental results at 4°C, where metabolic flux analysis, biomass characterization, and pool size measurements were performed: the ED pathway is the main glycolytic route, the biomass contains a large portion of ash (20%, inorganic salts), and the pool size of energy molecules is small (relative to normal-growth *E. coli* at 37°C). The right side shows experimental results at 23°C, where comparative RNA-Seq (between 4°C and 23°C) and dynamic isotopic carbon tracing were performed: the majority of genes were down-regulated after 2 hours of heat stress; and TCA cycle activity was limited compared to normal-growth conditions. After 24 hours, a shutdown of metabolic activity was observed, as cellular damage ensued.

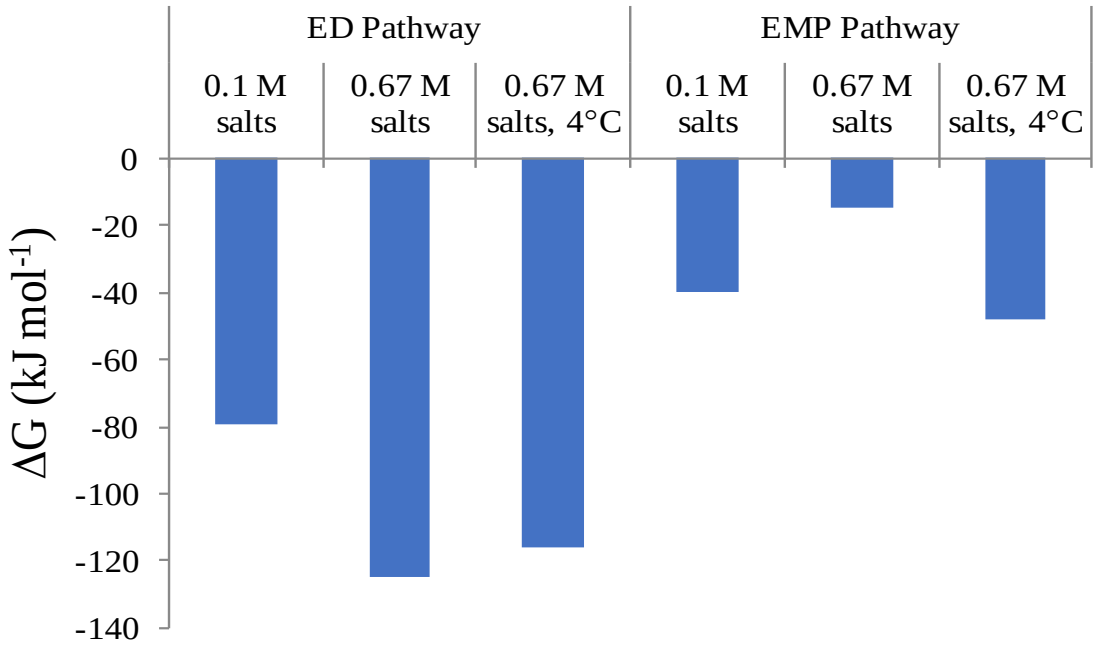

Fig. S6. Estimated changes in total Gibbs free energy (ΔG) for the conversion of glucose to pyruvate by the ED and EMP pathways under different inorganic salt and temperature conditions. Calculations were performed using the equilibrator calculator with reactant concentrations of 1 mM and a pH of 7.5.

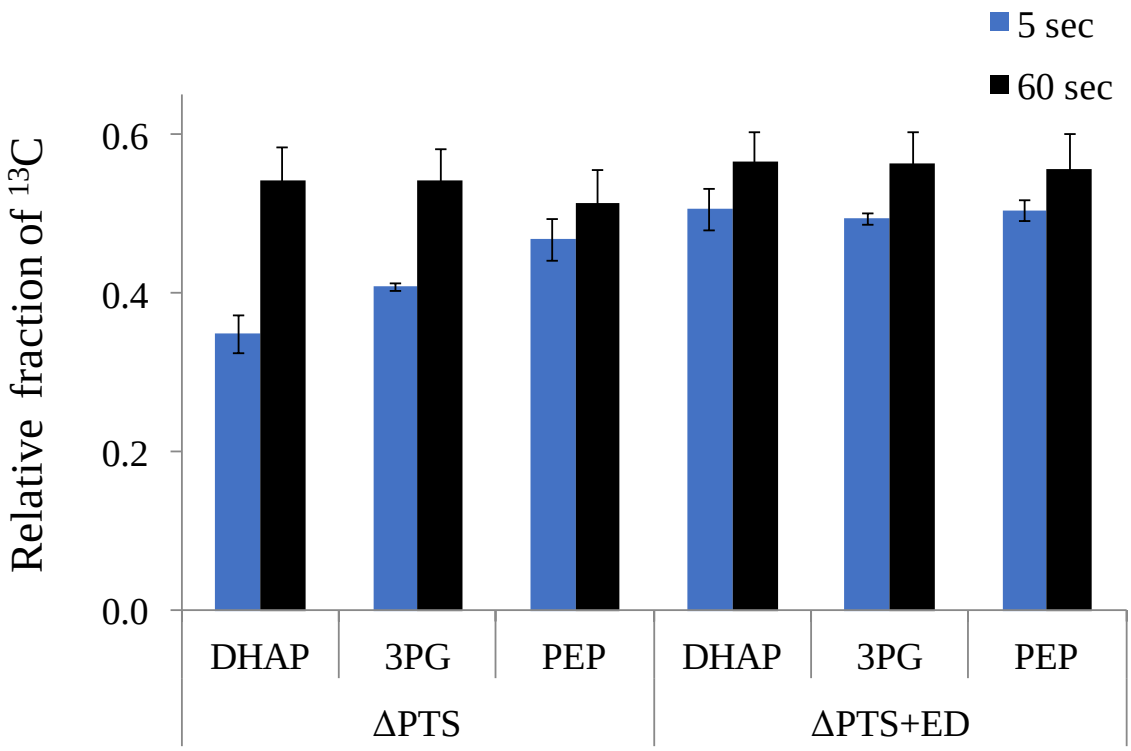

Fig. S7. Dynamic labeling experiments conducted with Δ*ptsG* and Δ*ptsG* + ED pathway overexpressing *E. coli* mutants following a U-^{13}C glucose pulse at 4°C. Direct product of the ED pathway is glyceraldehyde 3-phosphate (which quickly isomerizes to DHAP). Error bars indicate standard deviation of the mean (n = 2).

Table S1. MFA metabolic network and flux results

WuFlux reaction number	Reaction	Glucose flux results	Glucose confidence interval	Lactate flux results	Lactate confidence interval
1	Glucose(substrate) + ATP == G6P	100	-*	0	-*
2	G6P == F6P	2.94	1.93	–10.90	4.28
3	F6P + ATP == FBP	100.39	1.94	65.16	17.62
4	FBP == F6P	100.00	1.56	75.14	16.80
6	FBP == DHAP + GAP	0.39	0.40	–9.98	2.27
7	DHAP == GAP	0.39	0.40	–9.98	2.27
8	GAP == G3P + ATP + NADH	88.73	0.47	–14.95	2.23
9	G3P == PEP	79.94	0.57	–20.42	2.34
10	PEP == PYR + ATP	70.61	5.40	40.41	12.78
11	Lactate(Substrate) == PYR + NADH		-*	100	-*
12	PYR + 2*ATP == PEP	2.08	1.69	23.79	9.01
14	PYR == AceCoA + CO2 + NADH	142.61	2.61	76.36	1.68
15	AceCoA + OAA == CIT	128.28	1.09	60.57	3.40
16	CIT == ICIT	128.28	1.09	60.57	3.40
17	ICIT == AKG + CO2 + NADPH	128.28	1.91	53.78	5.86
18	AKG == SucCoA + CO2 + NADH	124.26	1.93	51.36	6.09
19	SucCoA == SUC + ATP	122.55	1.93	50.33	6.17
20	SUC == FUM + FADH2	124.26	1.13	58.15	3.64
21	FUM == MAL	125.47	1.11	58.88	3.56
22	MAL == OAA + NADH	44.34	11.65	62.09	7.63
23	MAL == PYR + CO2 + NADH	26.83	9.24	3.10	4.46
24	MAL == PYR + CO2 + NADPH	54.30	7.42	0.48	5.05
25	PEP + CO2 == OAA	8.47	5.29	0.34	25.51
26	OAA + ATP == PEP + CO2	0.00	1.57	39.16	19.46

27	PYR + ATP + CO2 == OAA	86.08	9.14	43.29	9.69
28	ICIT == GLX + SUC	0.00	1.75	6.79	2.80
29	GLX + AceCoA == MAL	0.00	1.75	6.79	2.80
30	G6P == PG6 + NADPH	95.72	1.94	10.10	4.30
31	PG6 == CO2 + Ru5P + NADPH	7.22	2.44	4.96	3.56
33	Ru5P == X5P	1.22	1.64	1.15	2.48
34	Ru5P == R5P	6.00	0.81	3.82	1.19
35	X5P + R5P == GAP + S7P	1.28	0.82	0.98	1.21
36	GAP + S7P == E4P + F6P	1.28	0.82	0.98	1.21
37	X5P + E4P == GAP + F6P	-0.06	0.83	0.17	1.26
38	PG6 == PYR + GAP	88.50	0.94	5.13	2.17
40	AceCoA == Ac + ATP	–1.46	0.02	–0.88	0.09
41	AKG + NADPH == GLU	27.11	0.37	16.11	1.76
42	GLU + ATP == GLN	2.45	0.03	1.47	0.16
43	GLU + ATP + 2*NADPH == PRO	0.70	0.01	0.42	0.04
44	GLU + GLN + CO2 + ASP + AceCoA + 5*ATP + NADPH == ARG + AKG + FUM + Ac	0.76	0.01	0.46	0.05
45	OAA + GLU == ASP + AKG	8.80	0.35	4.91	0.74
46	ASP + 2*ATP == ASN	1.01	0.01	0.61	0.06
47	PYR + GLU == ALA + AKG	1.91	0.02	1.15	0.12
48	G3P + GLU == SER + AKG + NADH	5.48	0.17	3.49	0.39
49	SER == GLY + Methylene_THF	3.64	0.17	2.38	0.30

50	GLY == Methylene_THF + CO2 + NADH	1.43	0.17	0.67	0.25
51	Methylene_THF + NADH == Methyl_THF	0.44	0.01	0.27	0.03
52	Methylene_THF == Formyl_THF + NADPH	0.44	0.01	0.27	0.03
53	ASP + 2*ATP + 2*NADPH == THR	3.85	0.33	1.93	0.53
54	THR == GLY + AceCoA + NADH	1.69	0.33	0.63	0.47
55	SER + AceCoA + 3*ATP + 4*NADPH == CYS + Ac	0.70	0.01	0.42	0.04
56	ASP + PYR + GLU + SucCoA + ATP + 2*NADPH == LYS + CO2 + AKG + SUC	1.27	0.02	0.76	0.08
57	ASP + Methyl_THF + CYS + SucCoA + ATP + 2*NADPH == MET + PYR + SUC	0.44	0.01	0.27	0.03
58	GLU + NADPH + 2*PYR == VAL + AKG + CO2	1.27	0.02	0.76	0.08
59	AceCoA + 2*PYR + GLU + NADPH == LEU + AKG + NADH + 2*CO2	1.46	0.02	0.88	0.09
60	THR + PYR + GLU + NADPH == ILE + AKG + CO2	1.01	0.01	0.61	0.06
61	E4P + 2*PEP + GLU + ATP + NADPH == PHE + AKG + CO2	0.70	0.01	0.42	0.04
62	E4P + 2*PEP + GLU + ATP + NADPH == TYR	0.44	0.01	0.27	0.03

	+ AKG + NADH + CO2				
63	SER + R5P + 2*PEP + E4P + GLN + 3*ATP + NADPH == TRP + GAP + PYR + GLU + CO2	0.19	0.00	0.12	0.01
66	R5P + Formyl_THF + GLN + ASP + 5*ATP == HIS + AKG + FUM + 2*NADH	0.44	0.01	0.27	0.03
67	NADH == NADPH	–209.06	8.70	–24.30	14.72
68	NADH == 3*ATP	654.55	3.88	313.13	20.60
69	FADH2 == 2*ATP	124.26	1.13	58.15	3.64
71	ATP == ATP_maintenance	2000.00	1.93	814.79	66.28
72	CO2 == CO2_ex	397.43	2.19	190.47	11.62
74	Biomass formation†	5.34	0.06	3.21	0.34
75	Exchange coefficient of Reaction:G6P == F6P	0.11	0.06	0.56	0.20
76	Exchange coefficient of Reaction:FBP == DHAP + GAP	0.00	0.25	0.44	0.25
77	Exchange coefficient of Reaction:DHAP == GAP	0.18	0.19	0.99	0.23
78	Exchange coefficient of Reaction:GAP == G3P + ATP + NADH	1.00	0.26	0.08	0.26
79	Exchange coefficient of Reaction:G3P == PEP	1.00	0.19	1.00	0.25
80	Exchange coefficient of Reaction:CIT == ICIT	0.50	0.05	0.60	0.10
81	Exchange coefficient of Reaction:ICIT == AKG + CO2 + NADPH	0.28	0.25	0.00	0.00
82	Exchange coefficient of Reaction:SucCoA == SUC + ATP	0.32	0.16	0.60	0.23

83	Exchange coefficient of Reaction:SUC == FUM + FADH2	0.36	0.16	0.42	0.23
84	Exchange coefficient of Reaction:FUM == MAL	0.81	0.08	1.00	0.04
85	Exchange coefficient of Reaction:MAL == OAA + NADH	1.00	0.01	1.00	0.06
86	Exchange coefficient of Reaction:PYR + ATP + CO2 == OAA	0.00	0.02	0.00	0.00
87	Exchange coefficient of Reaction:Ru5P == X5P	0.00	0.00	0.52	0.25
88	Exchange coefficient of Reaction:Ru5P == R5P	1.00	0.26	0.58	0.25
89	Exchange coefficient of Reaction:X5P + R5P == GAP + S7P	0.99	0.23	0.04	0.26
90	Exchange coefficient of Reaction:GAP + S7P == E4P + F6P	0.07	0.24	0.39	0.26
91	Exchange coefficient of Reaction:X5P + E4P == GAP + F6P	1.00	0.25	0.09	0.25
92	Exchange coefficient of Reaction:SER == GLY + Methylene_THF	0.08	0.09	0.05	0.02
93	Exchange coefficient of Reaction:GLY == Methylene_THF + CO2 + NADH	0.00	0.00	0.00	0.00
94	Intracellular 13CO_2 fraction	0.40	0.00	0.24	0.01
95	SSR (95% CI)	93.19	76.8–133.0	67.89	48.8–95.0

*Flux values were set manually in each situation to represent glucose or lactate uptake. Thus, no confidence intervals are provided.

†Biomass formulation equation =
0.357*ALA+0.143*ARG+0.19*ASN+0.19*ASP+0.048*CYS+0.196*GLU+0.196*GLN+0.729*GLY+0.083*HIS+0.19*ILE+0.274*LEU+0.238*LYS+0.083*MET+0.131*PHE+0.131*PRO+0.179*SER+0.214*THR+0.036*TRP+0.083*TYR+0.238*VAL+0.25*G6P+0.706*F6P+0.766*R5P+0.129*GAP+0.619*G3P+0.051*PEP+0.083*PYR+2.725*AceCoA+0.087*AKG+0.340*OAA+0.783*Methylene_THF+33.247*ATP+5.363*NADPH==39.68*Biomass+1.455*NADH

Additional data table S1. (XLS)

Dataset S1: Mass isotopomer distribution data from steady state and dynamic flux analysis

Additional data table S2. (XLS)

Dataset S2: RNA sequencing data

References

1. Abernathy MH, et al. (2017) Deciphering cyanobacterial phenotypes for fast photoautotrophic growth via isotopically nonstationary metabolic flux analysis. *Biotechnol Biofuels* 10:273 https://doi.org/10.1186/s13068-017-0958-y.
2.. Ma F, Jazmin JL, Young, JD, Allen DK (2014) Isotopically nonstationary 13C flux analysis of changes in *Arabidopsis thaliana* leaf metabolism due to high light acclimation. *Proc Natl Acad Sci U S A* 111(47):16967-16972.
3. Pramanik J, Keasling JD (1997) Stoichiometric model of *Escherichia coli* metabolism: incorporation of growth-rate dependent biomass composition and mechanistic energy requirements. *Biotechnol Bioeng* 56(4):398–421.
4. Pramanik J, Keasling JD (1998) Effect of *Escherichia coli* biomass composition on central metabolic fluxes predicted by a stoichiometric model. *Biotechnol Bioeng* 60(2):230–238.
5. Neidhardt FC, Ingraham JL, Schaechter M (1990) *Physiology of the Bacterial Cell:A Molecular Approach* (Sinauer Associates, Sunderland, MA), pp xii, 506 p.